

# Propagation in Graded Index (GI) Optical Fibres

HTE - 24.02.2013

## 1. Graded Index Fibre

As shown in Fig. 2.2, the refractive index of the core will change with radial distance in graded index fibre. To reflect this profile variation, we write as follows

$$n(r) = n_1 \left[ 1 - 2\Delta \left( \frac{r}{a} \right)^q \right]^{0.5}, \quad n(r_n) = n_1 (1 - 2\Delta r_n^q)^{0.5} \quad \text{when } 0 \leq r \leq a \quad \text{or} \quad 0 \leq r_n \leq 1$$

$$n(r) = n_1 (1 - 2\Delta)^{0.5} \approx n_1 (1 - \Delta) = n_2 \quad \text{when } r > a \quad \text{or} \quad r_n > 1 \quad (1.1)$$

A typical variation of  $n(r_n)$  against  $r_n$  (the normalized radial distance) at selected values of  $q$ , called the grading parameter, is shown in Fig. 1.1.

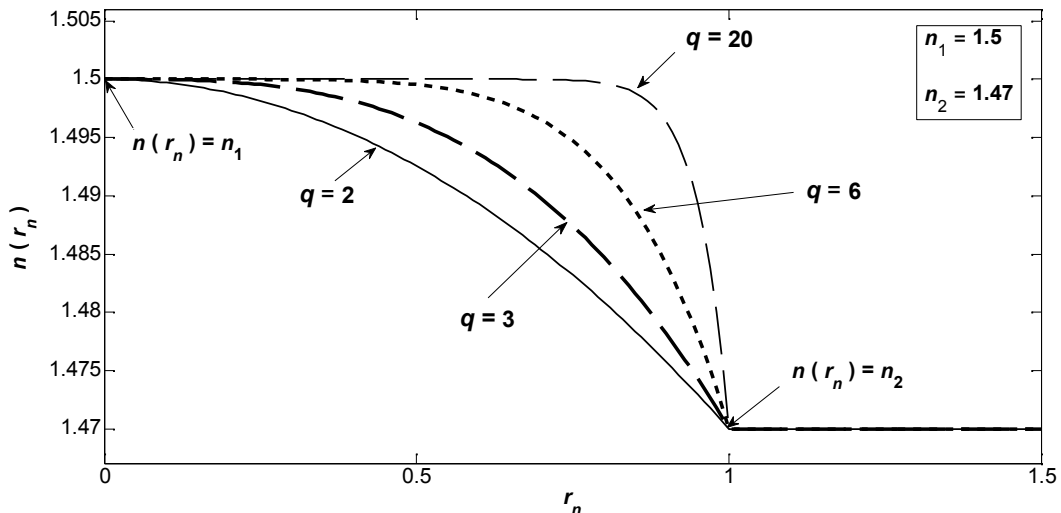


Fig. 1.1 Variation of fibre refractive index profile against radial distance at selected values of the grading parameter.

From Fig. 1.1, we understand that, as  $q \rightarrow \infty$ , the refractive index profile will approximate to step index case. In practice, the mostly used value of the grading parameter is  $q = 2$ . We further note from (1.1) and Fig. (1.1) that in graded index fibres  $n_1$  is becomes the refractive index value only at core centre (i.e. fibre axis), whereas in step index multi mode or single mode,  $n_1$  is known as the core refractive index.

It is important to realize that, the ray trajectories (the path followed by the ray when propagating along the fibre axis) in graded index fibres will be different from that of step index fibres. This is because, in a step index fibre, every ray will have to go as far as the core cladding boundary, before it

bends (gets reflected) back into the fibre core. Keeping in mind the refractive index profile variation in Fig. 1.1, the rays propagating in a graded index fibre, will face refraction continuously at all radial positions. Now imagine a propagating ray that starts its journey from around the fibre axis and moves towards the cladding. Since the refractive index becomes lower as the radial position increases (i.e. as we get closer to the cladding boundary), each time the ray refracts, it will form a smaller angle with fibre axis (greater angle with the line of normal). Eventually, the ray will experience total internal reflection and will bend towards the fibre axis again. This is shown in an exaggerated manner in Fig. 1.2 together with the propagation of a ray in step index fibre. Bear in mind that Fig. 1.2 is a two dimensional view. In the next section we examine this situation in three dimensions and deduce the related numerical aperture formulations and arrive at the classification of rays as meridional and skew.

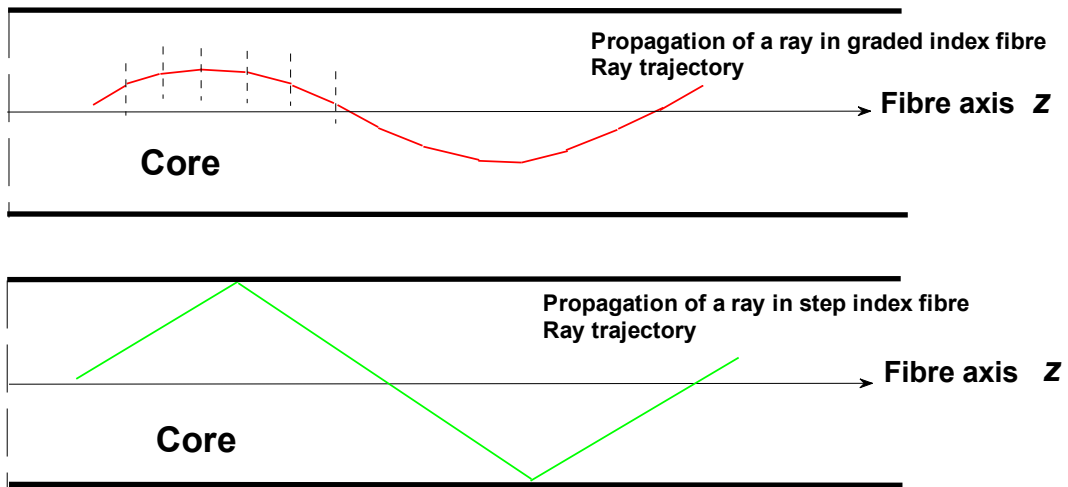


Fig. 1.2 Typical ray trajectories in graded index and step index fibres in two dimensional view.

## 2. Derivation of Ray Path (Ray Trajectory)

According to Fermat's principle, in a medium with a refractive index  $n(\mathbf{R})$ , the ray path,  $s$  followed by the ray is described by

$$\frac{d}{ds} \left[ n(\mathbf{R}) \frac{d\mathbf{R}}{ds} \right] = \nabla n(\mathbf{R}) \quad (2.1)$$

where in Cartesian coordinates,  $\mathbf{R} = (x, y, z)$ . A simplified illustration is given in Fig. 2.1.

As shown in Fig. 2.1, the ray propagates from a point  $A$  (which is made coincident with the origin of the coordinate system) to a point  $B$ , following a curved path due to refractive index changes along  $x, y, z$  axes.

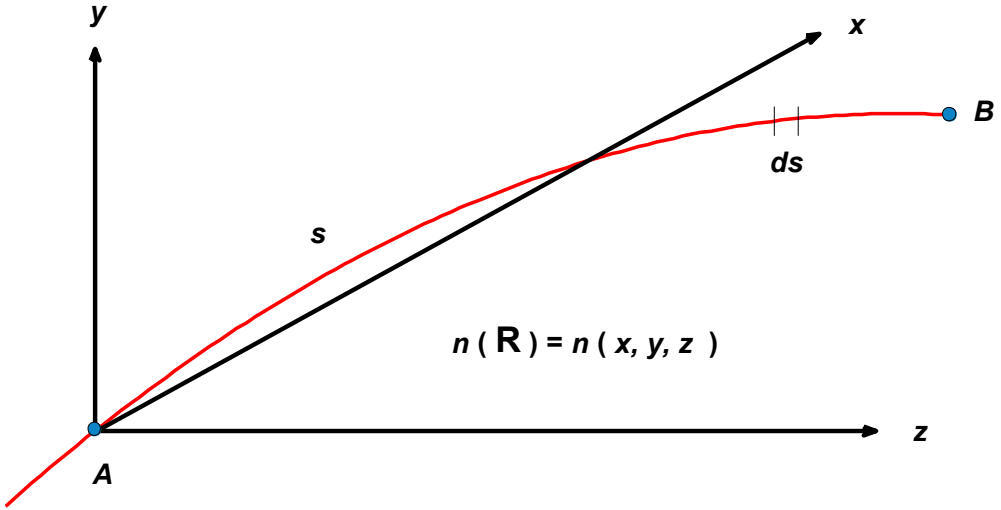


Fig. 2.1 A simplified illustration of a ray path in medium of refractive index  $n(\mathbf{R})$ .

By noting that

$$\nabla = \frac{\partial}{\partial x} + \frac{\partial}{\partial y} + \frac{\partial}{\partial z} \quad (2.2)$$

We can split (2.1) into separate  $x$ ,  $y$ ,  $z$  axes, then we get

$$\frac{d}{ds} \left[ n(\mathbf{R}) \frac{dx}{ds} \right] = \frac{\partial}{\partial x} n(\mathbf{R}), \quad \frac{d}{ds} \left[ n(\mathbf{R}) \frac{dy}{ds} \right] = \frac{\partial}{\partial y} n(\mathbf{R}), \quad \frac{d}{ds} \left[ n(\mathbf{R}) \frac{dz}{ds} \right] = \frac{\partial}{\partial z} n(\mathbf{R}) \quad (2.3)$$

(2.3) means that we have transformed the ray path dependence into  $x$ ,  $y$ ,  $z$  components, thus it is reasonable to write

$$x = x(s), \quad y = y(s), \quad z = z(s) \quad (2.4)$$

Additionally, we can define the followings

$$ds^2 = dx^2 + dy^2 + dz^2, \quad ds = dz \left[ 1 + \left( \frac{dx}{dz} \right)^2 + \left( \frac{dy}{dz} \right)^2 \right]^{0.5} = dz \sqrt{1 + \left( \frac{dx}{dz} \right)^2 + \left( \frac{dy}{dz} \right)^2} \quad (2.5)$$

In fibres, propagation is almost parallel to  $z$  axis, since the refractive index difference between core and cladding is quite small. Therefore we can safely say that rays mostly propagate parallel to  $z$  axis, allowing us to make the following approximation

$$s \approx z, \quad ds \approx dz, \quad \frac{dz}{ds} \approx 1 \quad (2.6)$$

Then the third differential equation (DE) in (2.3) will turn into

$$\frac{d}{ds} \left[ n(\mathbf{R}) \frac{dz}{ds} \right] = \frac{\partial}{\partial z} n(\mathbf{R}) , \quad \frac{d}{ds} \left[ n(\mathbf{R}) \right] = \frac{\partial}{\partial z} n(\mathbf{R}) , \quad \frac{d}{ds} n(\mathbf{R}) = \frac{d}{ds} n(\mathbf{R}) \quad (2.7)$$

So this third DE is redundant and we are left with the first and the second DEs in (2.3). Applying the approximation of (2.6) to the remaining DEs, we get

$$\frac{d}{dz} \left[ n(\mathbf{R}) \frac{dx}{dz} \right] = \frac{\partial}{\partial x} n(\mathbf{R}) , \quad \frac{d}{dz} \left[ n(\mathbf{R}) \frac{dy}{dz} \right] = \frac{\partial}{\partial y} n(\mathbf{R}) \quad (2.8)$$

In solving (2.8) initially we take the simplest case of

$$n(\mathbf{R}) = n(x, y, z) = n \quad (2.9)$$

which implies that the medium of propagation is completely homogeneous, thus there is no refractive index variation along  $x, y, z$ , i.e. the refractive index remains constant whatever  $x, y, z$  coordinate values are. Then (2.8) will be

$$\frac{d}{dz} \left[ n(\mathbf{R}) \frac{dx}{dz} \right] = \frac{d^2 x}{dz^2} = 0 , \quad \frac{d}{dz} \left[ n(\mathbf{R}) \frac{dy}{dz} \right] = \frac{d^2 y}{dz^2} = 0 \quad (2.10)$$

The solutions to (2.10) are simple straight lines given by

$$x = x(s) = A_x z + A_{x0} , \quad y = y(s) = A_y z + A_{y0} \quad (2.11)$$

where  $A_x, A_{x0}, A_y, A_{y0}$  are determined from the initial conditions such that

$$\left. \frac{dx}{dz} \right|_{z=0} = A_x , \quad x|_{z=0} = A_{x0} , \quad \left. \frac{dy}{dz} \right|_{z=0} = A_y , \quad y|_{z=0} = A_{y0} \quad (2.12)$$

which means that when the ray starts its journey at  $z = 0$ , it is at the initial  $x, y$  coordinates of  $A_{x0}, A_{y0}$  and it has the slopes (the tangent of the angles) of  $A_x, A_y$  with respect to  $x, y$  axes. A corresponding plot is given in Fig. 2.2. In this figure, there is actually a third angle which should be defined with respect to  $z$  axis, but this is not marked, since this particular angle is nearly zero due to assumptions made in (2.6).

An important observation regarding Fig. 2.2 and the solutions in (2.10) is that in a medium where the refractive index is constant in all directions, the ray path is simply a straight line and the position of the ray at point  $B$  is simply determined by the initial conditions at  $A$ . This is not a surprising finding, since this is just a verification of a known fact.

Now applying (2.10) to (2.12) to step index (multimode fibre) we obtain the following for a ray propagating in the core

$$\begin{aligned} x = x(z) &= \theta_{x0} z + x_0 , \quad y = y(z) = \theta_{y0} z + y_0 \\ \left. \frac{dx}{dz} \right|_{z=0} &= \theta_{x0} , \quad x|_{z=0} = x_0 , \quad \left. \frac{dy}{dz} \right|_{z=0} = \theta_{y0} , \quad y|_{z=0} = y_0 \end{aligned} \quad (2.13)$$

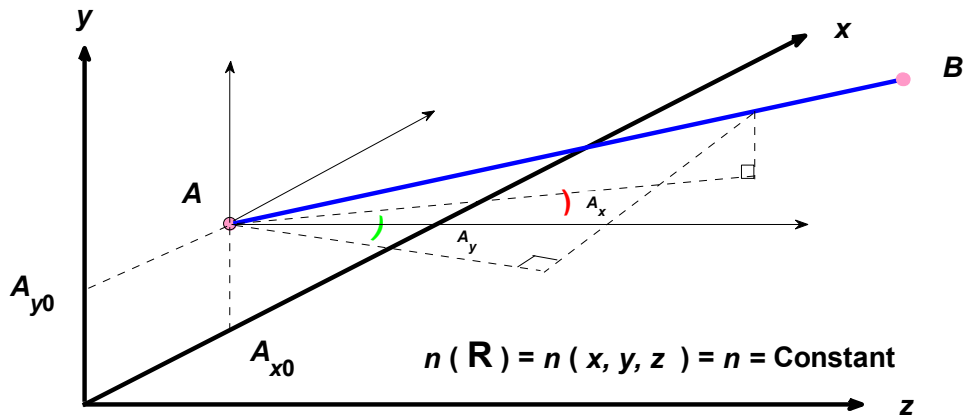


Fig. 2.2 Illustration of ray propagation in a medium of constant refractive index.

Note that we have slightly changed the notation in (2.13) to emphasize that it is for a step index (multimode fibre) fibre. It should also be noted that (2.13) does not cover the propagation in the cladding, since no related boundary conditions have been set.

The geometry describing (2.13) is drawn in Fig. 2.3.

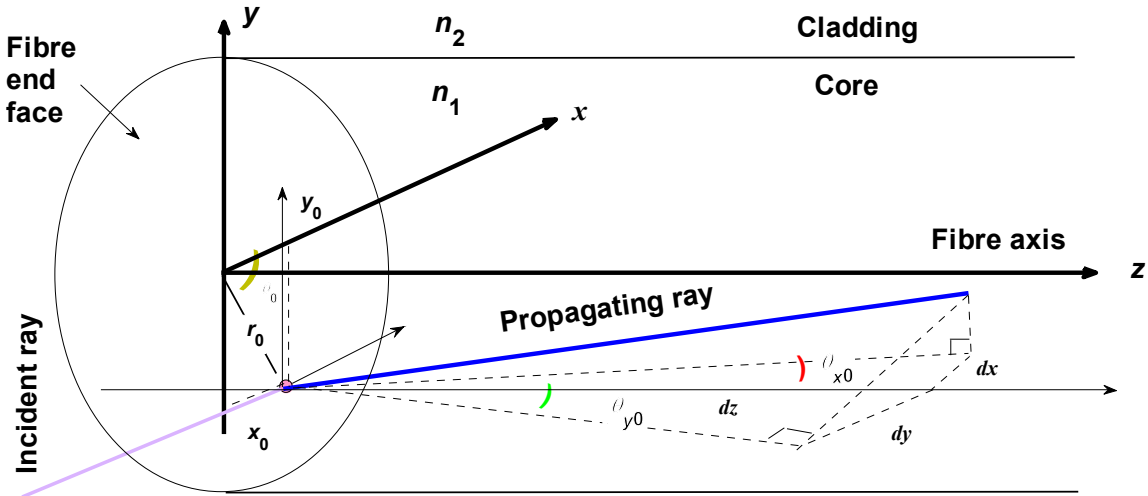


Fig. 2.3 The geometry describing ray entry and propagation in step index (multimode) fibre.

From Fig. 2.3, we identify that in line with the definition it is clear that two types of rays will exist in fibre

- a) Meridional Rays : These are rays with  $\theta_{x0} = \theta_{y0}$  and  $x_0 = y_0$  or any  $\theta_{x0}, \theta_{y0}$  with  $x_0 = y_0 = 0$ , In this case, the projection of the ray path onto any  $xy$  plane cross section (or fibre end face) passes through the fibre axis, i.e.  $r = 0$  .

b) Skew Rays : These are rays with  $\theta_{x_0} \neq \theta_{y_0}$  or  $x_0 \neq y_0$ . This way, the ray trajectory projected onto fibre front face never passes through the fibre axis, i.e.  $r = 0$  .

The cross sectional views of the fibre for the trajectories of meridional and skew rays are shown in Fig. 2.4.

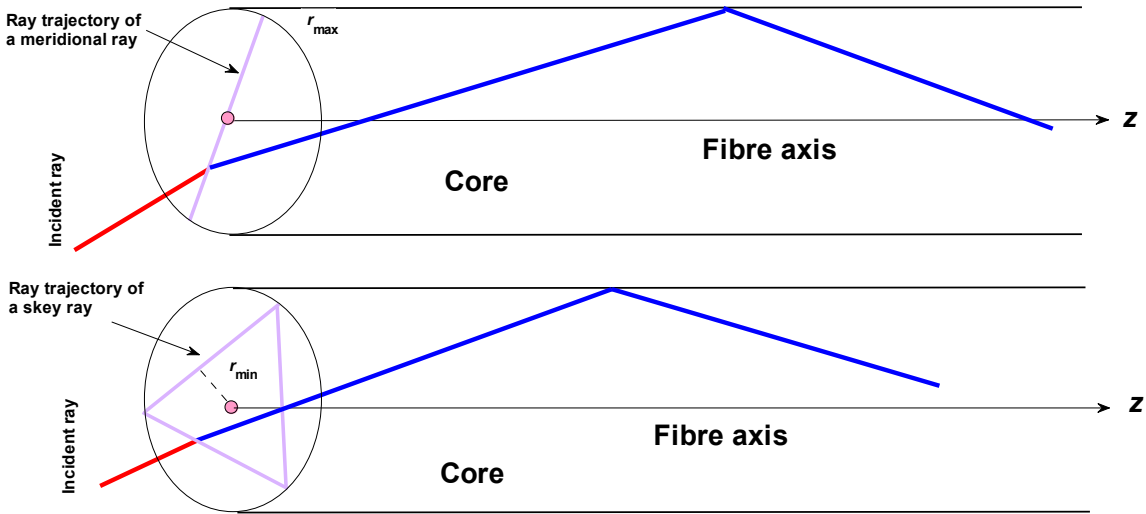


Fig. 2.4 Ray trajectories of meridional and skew ray in (multimode) step index fibre.

During their successive reflections from the core cladding boundary, skew rays will come close to the fibre the fibre axis, but never cross it. The closest the skew rays get to the fibre axis is known as  $r_{\min}$  . Of course, there is also  $r_{\max}$  , but in step (multimode) fibres, it is always the case that  $r_{\max} = a$  . There

Of course with the formulation of (2.8), it is more instructive to study the propagation in graded index fibres, since this is not covered as yet by mode analysis.

To this end, we take (1.1) and set  $q = 2$  , then convert the core refractive index variation into Cartesian coordinates as follows

$$n(r) = n_1 \left(1 - 2\Delta \frac{r^2}{a^2}\right)^{0.5}, \quad n(x, y) = n_1 \left(1 - 2\Delta \frac{x^2 + y^2}{a^2}\right)^{0.5}$$

$$n(x_n, y_n) = n_1 \left[1 - 2\Delta (x_n^2 + y_n^2)\right]^{0.5}, \quad x_n = x/a, \quad y_n = y/a \quad (2.14)$$

From (2.14), we try to write for  $n(x_n)$  or  $n(x)$  . We know that in fibres, the refractive index difference,  $\Delta$  is quite small, i.e.  $\Delta \ll 1$  , hence  $n(x)$  and  $n(y)$  can be retrieved from the last line of (2.14) as

$$n(x) \approx n_1 \left(1 - \Delta \frac{x^2}{a^2}\right), \quad n(y) \approx n_1 \left(1 - \Delta \frac{y^2}{a^2}\right) \quad (2.15)$$

Inserting the  $x$  part of (2.15) into (2.8), we get

$$\begin{aligned}
\frac{d}{dz} \left[ n(x) \frac{dx}{dz} \right] &= \frac{d}{dx} n(x) \quad , \quad \frac{d}{dz} \left[ n_1 \left( 1 - \Delta \frac{x^2}{a^2} \right) \frac{dx}{dz} \right] = \frac{d}{dx} n_1 \left( 1 - \Delta \frac{x^2}{a^2} \right) \\
\frac{dx}{dz} \frac{d}{dz} \left[ n_1 \left( 1 - \Delta \frac{x^2}{a^2} \right) \right] + n_1 \left( 1 - \Delta \frac{x^2}{a^2} \right) \frac{d^2 x}{dz^2} &= -2n_1 \Delta \frac{x}{a^2} \\
\frac{d^2 x}{dz^2} &\simeq -2\Delta \frac{x}{a^2} \quad , \quad \frac{d^2 y}{dz^2} \simeq -2\Delta \frac{y}{a^2}
\end{aligned} \tag{2.16}$$

In arriving at the last line (2.16), we have made the approximation  $1 - \Delta \frac{x^2}{a^2} \simeq 1$  and written the result for the  $y$  part by analogy of the  $x$  part.

The solutions to the second order DEs on the last line of (2.16) are sinusoidal functions, i.e. sines and cosines. Thus we adopt the following solutions

$$\begin{aligned}
x(z) &= A_x \cos \left( \frac{\sqrt{2\Delta}}{a} z \right) + B_x \sin \left( \frac{\sqrt{2\Delta}}{a} z \right) \\
y(z) &= A_y \cos \left( \frac{\sqrt{2\Delta}}{a} z \right) + B_y \sin \left( \frac{\sqrt{2\Delta}}{a} z \right)
\end{aligned} \tag{2.17}$$

where the terms  $A_x, B_x, A_y, B_y$  are to be determined by the initial conditions at  $z = 0$ , also called launching conditions. Assuming that these initial conditions are

$$\left. \frac{dx}{dz} \right|_{z=0} = \theta_{x0} \quad , \quad x|_{z=0} = x_0 \quad , \quad \left. \frac{dy}{dz} \right|_{z=0} = \theta_{y0} \quad , \quad y|_{z=0} = y_0 \tag{2.18}$$

in which case  $A_x, B_x, A_y, B_y$  will become

$$A_x = x_0 \quad , \quad A_y = y_0 \quad , \quad B_x = \frac{a\theta_{x0}}{\sqrt{2\Delta}} \quad , \quad B_y = \frac{a\theta_{y0}}{\sqrt{2\Delta}} \tag{2.19}$$

Inserting (2.19) into (2.17), we get finally the equations that describe the ray trajectory (ray path) in  $x$  and  $y$  as the ray propagates along the  $z$  in a graded index fibre, hence

$$\begin{aligned}
x(z) &= x_0 \cos \left( \frac{\sqrt{2\Delta}}{a} z \right) + \frac{a\theta_{x0}}{\sqrt{2\Delta}} \sin \left( \frac{\sqrt{2\Delta}}{a} z \right) \\
y(z) &= y_0 \cos \left( \frac{\sqrt{2\Delta}}{a} z \right) + \frac{a\theta_{y0}}{\sqrt{2\Delta}} \sin \left( \frac{\sqrt{2\Delta}}{a} z \right)
\end{aligned} \tag{2.20}$$

By converting (2.20) to the radial coordinates, we obtain

$$\begin{aligned}
r(z) &= [x^2(z) + y^2(z)]^{0.5} \\
r(z) &= [(x_0^2 + y_0^2) \cos^2 \left( \frac{\sqrt{2\Delta}}{a} z \right) + \frac{a^2 (\theta_{x0}^2 + \theta_{y0}^2)}{2\Delta} \sin^2 \left( \frac{\sqrt{2\Delta}}{a} z \right) \\
&\quad + \frac{x_0 a \theta_{x0}}{\sqrt{2\Delta}} \sin \left( \frac{2\sqrt{2\Delta}}{a} z \right) + \frac{y_0 a \theta_{y0}}{\sqrt{2\Delta}} \sin \left( \frac{2\sqrt{2\Delta}}{a} z \right)]^{0.5}
\end{aligned} \tag{2.21}$$

(2.20) and (2.21) indicate that in graded index fibres, the ray path will no longer be straight lines but will be in some sinusoidal form as drawn in Fig. 1.2. In particular, for meridional rays, the ray path projection on the fibre cross section will be a straight line like shown in Fig. 2.4, but it will be helical for skew rays as demonstrated in the following example.

**Example 2.1 :** In this example with the help of Matlab file, Ray\_Tracing\_GI\_Exp4.m, we try to obtain the ray path as given by (2.20) and (2.21) and classify rays as meridional and skew, depending on the initial launching conditions given in (2.18) defined. We remind and formalize the classification given (in the context of step index fibres) above as follows

$$\begin{aligned}
\text{Meridional rays : } &\theta_{x0} = \theta_{y0} \text{ and } x_0 = y_0 \quad \text{or} \quad \text{any } \theta_{x0}, \theta_{y0} \text{ with } x_0 = y_0 = 0 \\
\text{Skew rays : } &\text{any } \theta_{x0} \neq \theta_{y0} \quad \text{or} \quad \text{any } x_0 \neq y_0
\end{aligned} \tag{2.22}$$

By running Ray\_Tracing\_GI\_Exp4.m and taking sample graphical outputs, by setting  $\theta_{x0}$ ,  $\theta_{y0}$ ,  $x_0$ ,  $y_0$  for meridional and skew ray in conformance with (2.22), we obtain the following plots. Note that in these figures we have used the normalized versions of  $x_0$ ,  $y_0$  such that

$$x_{0n} = x_0 / a, y_{0n} = y_0 / a \tag{2.23}$$

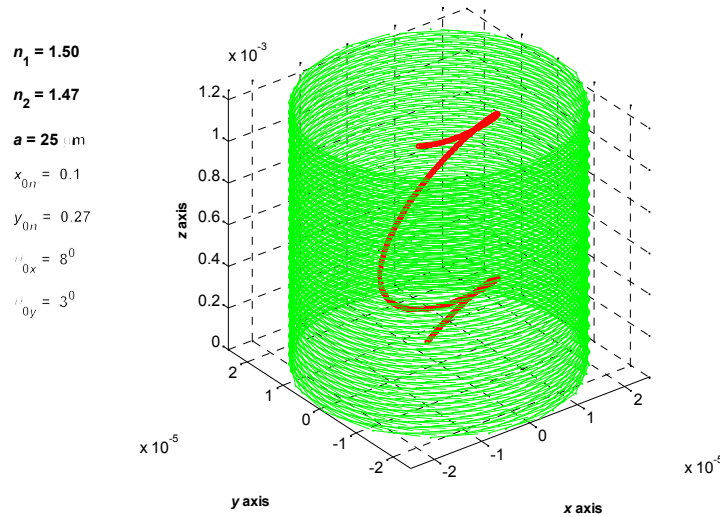


Fig. 2.5 Ray path (ray trajectory) of a skew ray of given initial launching conditions in graded index fibre.

The green boundary in Fig. 2.5 represents the fibre core cylinder, while the red curve inside corresponds to the ray path. As seen from Fig. 2.5, the given initial launching conditions define a skew ray, thus we observe in this figure a helical ray path. To view this path as it is projected onto the fibre cross section (or fibre front face), we simply rotate and get the view in Fig. 2.6

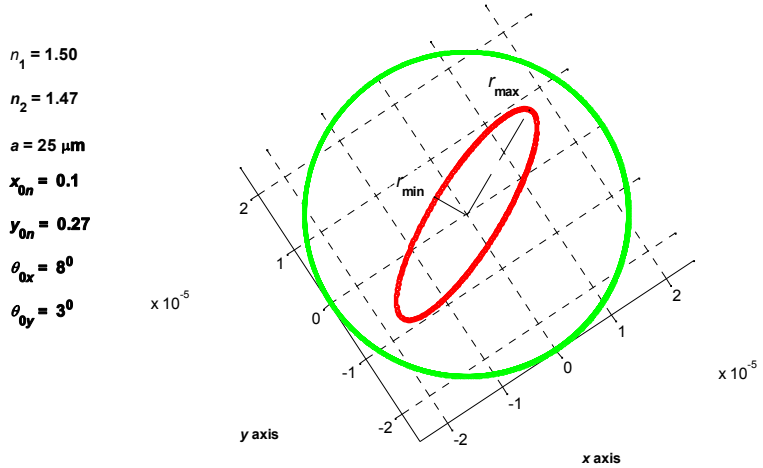


Fig. 2.6 Cross sectional view of Fig. 2.5.

In Fig. 2.6, it is possible to identify  $r_{\min}$  and  $r_{\max}$  respectively as the minor and the major axis of the parabola, traced by the projection of the skew ray path onto the cross section of the fibre.  $r_{\min}$  and  $r_{\max}$  respectively correspond to the radial distance that the ray gets closest to the fibre axis and the farthest distance that the moves away from the fibre axis.

Next, we exhibit the same plots for meridional rays. Figs. 2.7 and 2.8 are such examples.

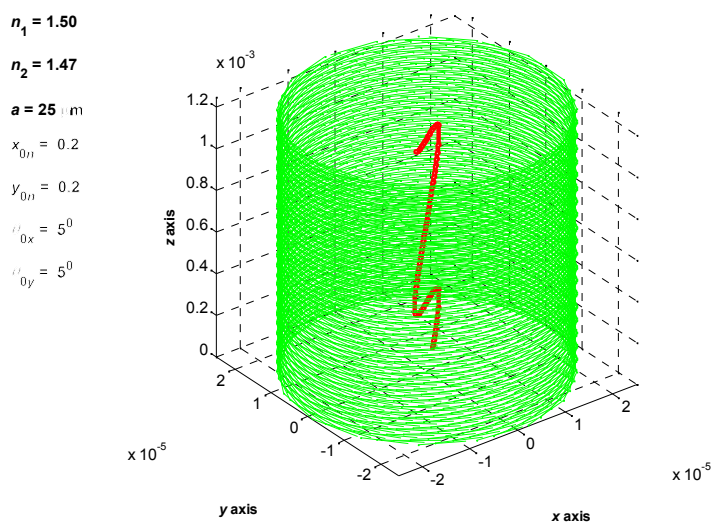


Fig. 2.7 Ray path (ray trajectory) of a typical meridional ray in graded index fibre.

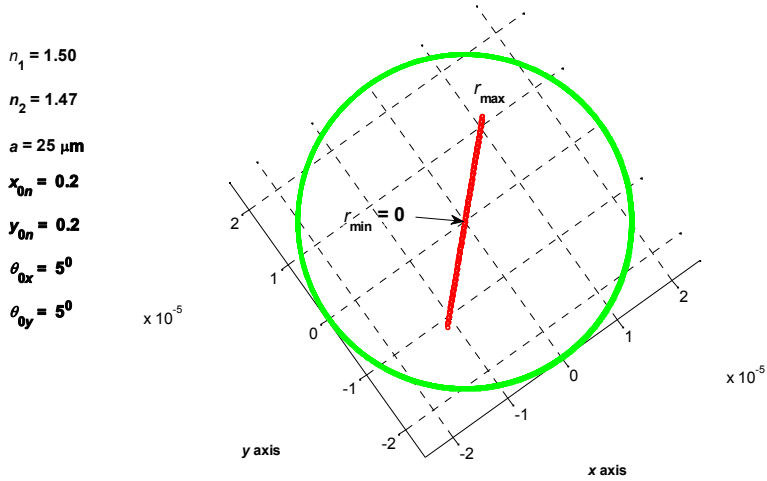


Fig. 2.8 Cross sectional view of Fig. 2.7.

As shown in Fig. 2.8, a meridional ray has  $r_{\min} = 0$ , this is no surprise since a meridional ray passes through fibre axis.

It is possible to obtain  $r_{\min}$  and  $r_{\max}$  by differentiating (2.21), finding the root of the resulting expression in terms of the  $z$  variable, finally by substituting this value back in (2.21). This procedure is explained below.

$$\begin{aligned} \frac{d}{dz} r(z) \rightarrow -\frac{\sqrt{2\Delta}}{a} (x_0^2 + y_0^2) \sin\left(\frac{\sqrt{2\Delta}}{a} z\right) + \frac{a}{\sqrt{2\Delta}} (\theta_{x0}^2 + \theta_{y0}^2) \sin\left(\frac{\sqrt{2\Delta}}{a} z\right) \\ + 2x_0 \theta_{x0} \cos\left(\frac{2\sqrt{2\Delta}}{a} z\right) + 2y_0 \theta_{y0} \cos\left(\frac{2\sqrt{2\Delta}}{a} z\right) = 0 \end{aligned} \quad (2.24)$$

After rearranging (2.24) and calling the root thus found  $z \rightarrow z_p$

$$z_p = \frac{a}{2\sqrt{2\Delta}} \tan^{-1} \left[ \frac{2a\sqrt{2\Delta}(x_0\theta_{x0} + y_0\theta_{y0})}{2\Delta(x_0^2 + y_0^2) - a^2(\theta_{x0}^2 + \theta_{y0}^2)} \right] \quad (2.25)$$

As illustrated by Figs. 2.5 and 2.7, the ray path is periodic, so we  $z_p$  can refer to the location  $r_{\min}$  or  $r_{\max}$ . Assuming that the  $z_p$  computed from (2.25) belongs to  $r_{\min}$  and we call it  $z_{p\min}$ , then  $z_{p\max}$  will be given by

$$\begin{aligned} z_{p\min} &= \frac{a}{2\sqrt{2\Delta}} \tan^{-1} \left[ \frac{2a\sqrt{2\Delta}(x_0\theta_{x0} + y_0\theta_{y0})}{2\Delta(x_0^2 + y_0^2) - a^2(\theta_{x0}^2 + \theta_{y0}^2)} \right] \\ z_{p\max} &= \frac{a}{2\sqrt{2\Delta}} \left\{ \tan^{-1} \left[ \frac{2a\sqrt{2\Delta}(x_0\theta_{x0} + y_0\theta_{y0})}{2\Delta(x_0^2 + y_0^2) - a^2(\theta_{x0}^2 + \theta_{y0}^2)} \right] + \pi \right\} \end{aligned} \quad (2.26)$$

Finally  $r_{\min}$  and  $r_{\max}$  will be obtained from

$$r_{\min} = [x^2(z_{p\min}) + y^2(z_{p\min})]^{0.5}, \quad r_{\max} = [x^2(z_{p\max}) + y^2(z_{p\max})]^{0.5} \quad (2.27)$$

**Example 2.2 :** In Matlab file, Ray\_Tracing\_GI\_Exp4.m ,  $r_{\min}$  and  $r_{\max}$  are calculated using (2.27) and printed out in the workspace. It is also possible to read these values by bringing data cursor onto the plot itself. This way we get the following figure

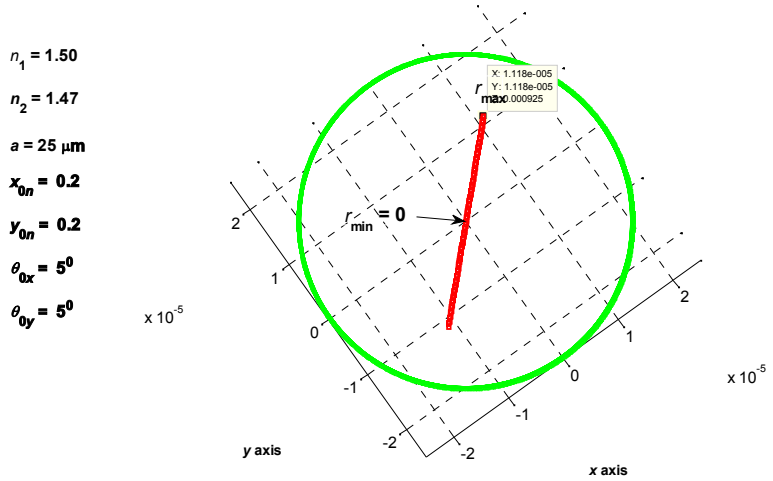


Fig. 2.9 The meridional ray projection of Fig. 2.8 with data cursor placed on  $r_{\max}$  .

In Fig. 2.8, our data cursor readings and the results of  $r_{\min}$  and  $r_{\max}$  printed out in the workspace are reproduced below.

In Fig. 2.9  $r_{\min} \approx 0$  and for  $r_{\max}$  :  $X = 11.18 \times 10^{-6}$  ,  $Y = 11.18 \times 10^{-6}$

$$r_{\max} = [X^2 + Y^2]^{0.5} = 15.81 \times 10^{-6}$$

From Matlab workspace :  $r_{\min} = 1.1979e-021$  ,  $r_{\max} = 1.5811e-005$       (2.28)

As seen (2.28), the two results and the labelling of  $r_{\min}$  and  $r_{\max}$  perfectly agree.

The equation on the left hand side of (2.27) can be used to check or broaden the definition of meridional rays, i.e. the set of  $\theta_{x0}$ ,  $\theta_{y0}$ ,  $x_0$ ,  $y_0$  that will yield the meridional ray condition of  $r_{\min} = 0$  . For this we simply solve the following

$$r_{\min} = [x^2(z_{p\min}) + y^2(z_{p\min})]^{0.5} = 0 \quad (2.29)$$

The solution of (2.29) delivers

$$x_0 \theta_{y0} = y_0 \theta_{x0} \quad (2.30)$$

It should be noted that (2.30) is a broader definition of meridional rays, since it also includes the ones given in (2.22).

For some of the settings of  $\theta_{x0}$ ,  $\theta_{y0}$ ,  $x_0$ ,  $y_0$ , we will inevitably get refracting rays, these rays are easily recognized on the plots of Matlab file, Ray\_Tracing\_GI\_Exp4.m, since for these rays,  $r_{\max} \geq a$ .

One such example is shown in Fig. 2.10, below.

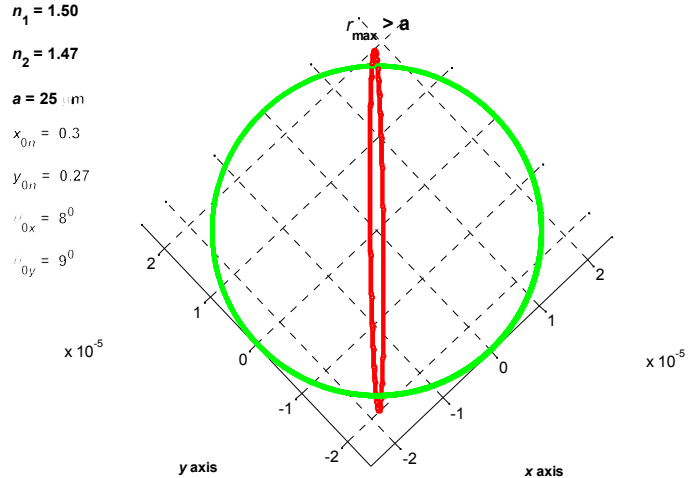


Fig. 2.10 The cross sectional view of a (skew) ray path with  $r_{\max} > a$ .

The reflection (or the refraction) of such rays from core cladding boundary cannot be exhibited by Ray\_Tracing\_GI\_Exp4.m, because the development that follows (2.16) does not take into account the boundary conditions of the core cladding interface.

Besides, the approximation in made in (2.6) ignores the angle of the ray path to the z axis, or rather assumes that it is zero. As seen from (2.5) to (2.9), this is not correct. On the other hand ray tracing in graded index medium or an exact solution of (2.3) is only possible by using numerical methods. Below we give a formulation, oriented at finding the numerical aperture (NA) in graded index fibres, which is taken from Ref. [4].

The light entrance into a fibre is shown in its most general form in Fig. 2.11. Benefiting from Ref. [4], we write the projection of the ray path on the fibre end face as

$$\frac{x^2}{T_x^2} + \frac{y^2}{T_y^2} = 1 \quad (2.31)$$

where  $T_x$  and  $T_y$  are defined as

$$\begin{aligned}
T_x &= \frac{4\Delta r_{0n}^2 (1-2\Delta r_{0n}^2) K^2}{1 - (1-2\Delta r_{0n}^2) \cos^2(\gamma_0) + \left\{ [1 - (1-2\Delta r_{0n}^2) \cos^2(\gamma_0)]^2 - 8\Delta r_{0n}^2 (1-2\Delta r_{0n}^2) K^2 \right\}^{0.5}} \\
T_y &= \frac{4\Delta r_{0n}^2 (1-2\Delta r_{0n}^2) K^2}{1 - (1-2\Delta r_{0n}^2) \cos^2(\gamma_0) - \left\{ [1 - (1-2\Delta r_{0n}^2) \cos^2(\gamma_0)]^2 - 8\Delta r_{0n}^2 (1-2\Delta r_{0n}^2) K^2 \right\}^{0.5}} \\
K &= \cos(\beta_0) \cos(\theta_0) - \cos(\alpha_0) \sin(\theta_0)
\end{aligned} \tag{2.32}$$

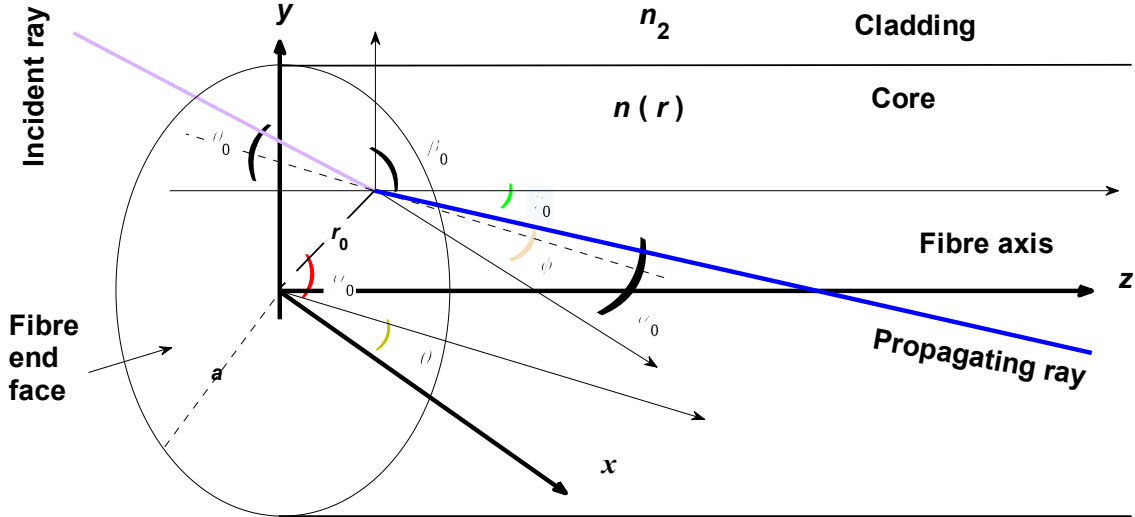


Fig. 2.11 The geometry describing ray entry in graded index fibre.

By plotting (2.31) for a set of input parameters, by observing the restriction

$$\cos^2(\alpha_0) + \cos^2(\beta_0) + \cos^2(\gamma_0) \leq 1 \tag{2.33}$$

we get the ellipse traced by ray path against the fibre cross section, this time without any approximations. Such a graphic is shown Fig. 2.12 for a skew ray. Note that here there is a tilt involved which is given by

$$T_\theta = \psi_0 + \frac{\pi}{4} - 0.5a \sin^{-1} \left\{ \frac{1 - (1-2\Delta r_{0n}^2) \cos^2(\gamma_0) - 4(1-2\Delta r_{0n}^2) K^2}{\left\{ [1 - (1-2\Delta r_{0n}^2) \cos^2(\gamma_0)]^2 - 8\Delta r_{0n}^2 (1-2\Delta r_{0n}^2) K^2 \right\}^{0.5}} \right\} \tag{2.34}$$

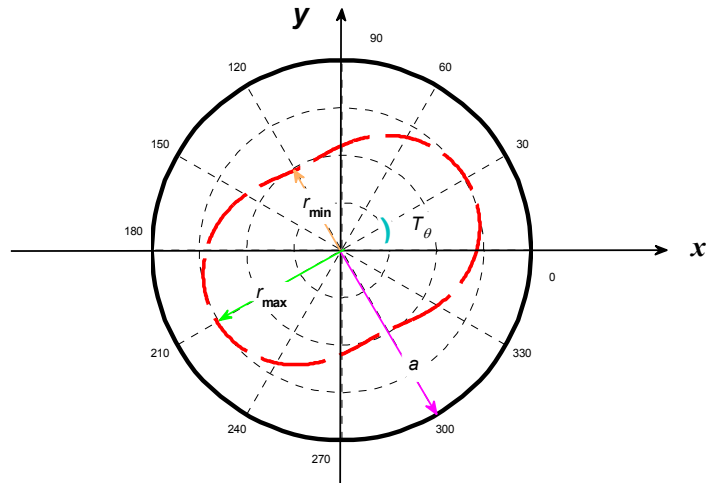


Fig. 2. 12 The cross sectional view of a (skew) ray path based on (2.31).

It is clear from Fig. (2.10) that the ray will be refracting if  $r_{\max} > a$ . In the case of (2.31), this boils down to the major axis (in this case, we take this as  $T_x$ ) being less than the fibre core radius, i.e.,

$$T_x \leq a \quad (2.35)$$

Using (2.35) in (2.32) and setting  $\psi_0 = 0$ , then in terms of the angle  $\phi$  which is the angle between the projection of the incident ray onto fibre end face and the  $x$  axis as shown Fig. 2.11, the numerical aperture of the graded index fibre will become

$$\text{NA}_{\text{GI}} = \sin(\theta_{0c}) = n_1 \left[ \frac{2\Delta(1-r_{0n}^2)}{1-r_{0n}^2 \cos^2(\phi)} \right]^{0.5} \quad (2.36)$$

It is worth noting that  $\phi$  is related to direction cosines of  $\alpha_0$  and  $\beta_0$  in the following manner

$$\frac{\cos^2(\alpha_0)}{\cos^2(\beta_0)} = \frac{1}{\sin^2(\phi)} - 1 \quad (2.37)$$

Since the most general incidence is examined in Fig. 2.11, the NA formulation given in (2.36) takes into account meridional as well as skew rays. As seen from Fig. 2.11,  $\phi$  is skewness angle such that

$$\begin{aligned} \text{For skew rays, } \phi &\neq \frac{\pi}{2} \text{ or } 90^\circ \\ \text{For meridional rays, } \phi &= \frac{\pi}{2} \text{ or } 90^\circ \end{aligned} \quad (2.38)$$

The NA of step index fibre incorporating meridional and skew rays is found to be

$$NA_{SI} = \sin(\theta_{0c}) = (n_1^2 - n_2^2)^{0.5} \left\{ 1 + \left[ \frac{r_{0n} \sin(\phi_i)}{1 + r_{0n} \cos(\phi_i)} \right]^2 \right\}^{0.5} \quad (2.39)$$

where  $\phi_i$  is given by

$$\phi_i = \cos^{-1}[-r_{0n} \cos(\phi)] + \phi \quad (2.40)$$

It is important to note that at the at the limit of  $\phi = \pi/2$ , i.e., at meridional ray limit,  $\phi_i$  of (2.40) assume the value of  $\phi_i = \pi$ , hence  $NA_{SI}$  defined in (2.39) becomes independent of  $r_{0n}$  and turns into (2.4) given in, "Notes on Fibre Propagation\_Jan 2013\_HTE" as shown below

$$NA_{SI} = (n_1^2 - n_2^2)^{0.5} = n_1 \sqrt{2\Delta} \quad (2.41)$$

The variation of the numerical aperture for graded and step index fibres are shown in Figs. 2.13 and 2.14 against the normalized radial distance at several skew angles.

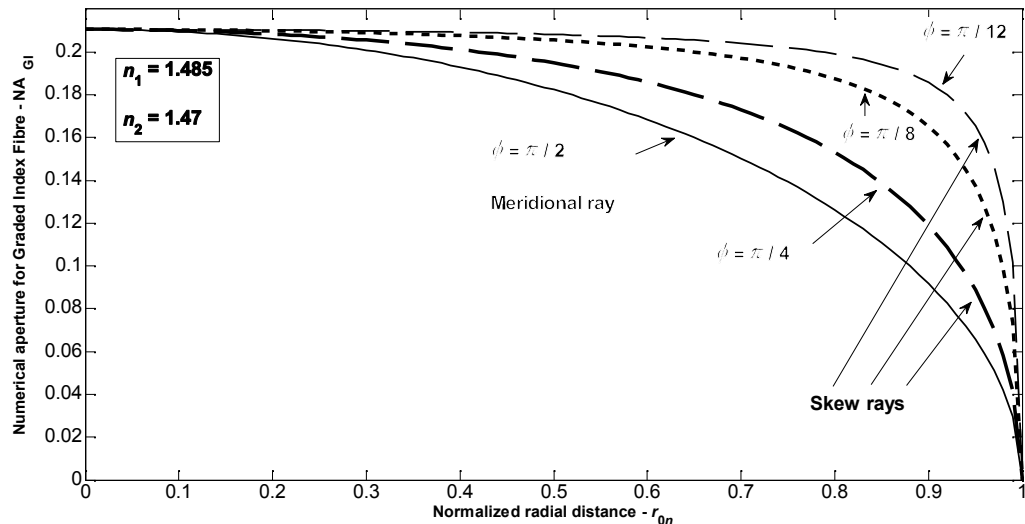


Fig. 2. 13 Numerical aperture variation of graded index fibre with normalized radial distance at different skew angles.

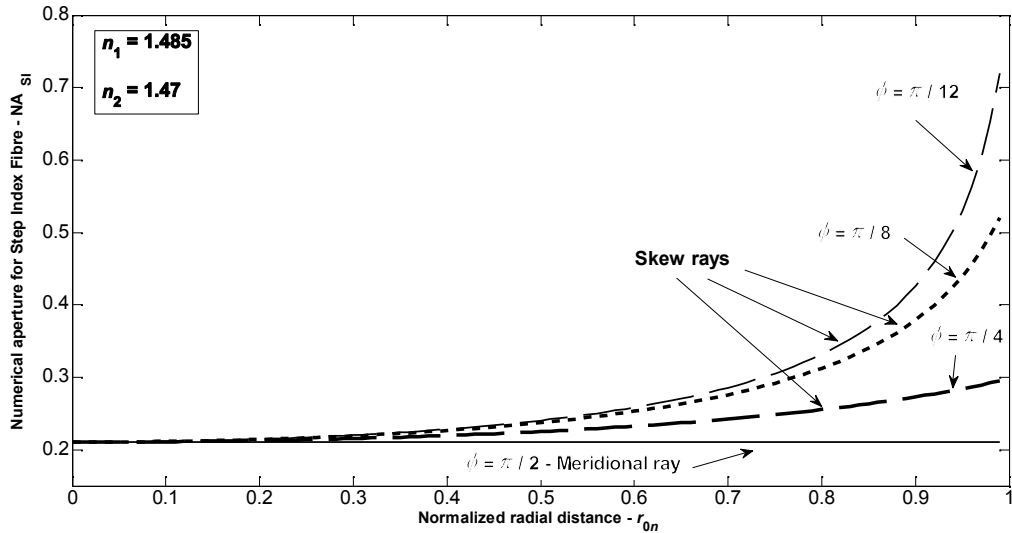


Fig. 2. 14 Numerical aperture variation of step index fibre with normalized radial distance at different skew angles.

As seen from Figs. 2.13 and 2.14, the acceptance cone for skew angles, i.e. the rays which have  $\phi \neq \pi/2$  is greater and it increases both with decreasing values of  $\phi$  and increasing values of  $r_{0n}$ . In step index fibre, as (2.39) and (2.40) reveal, theoretically the acceptance cone of the skew rays can go to infinity as we move towards the core cladding interface. But in graded index fibre, the acceptance cone cannot exceed that of the fibre axis, i.e. the numerical aperture at  $r_{0n} = 0$  as demonstrated by Fig. 2. 13. Viewed across a plane passing through the fibre axis (side view), the cases depicted in Figs. 2.13 and 2.14 will look like the ones shown in Fig. 2.15.

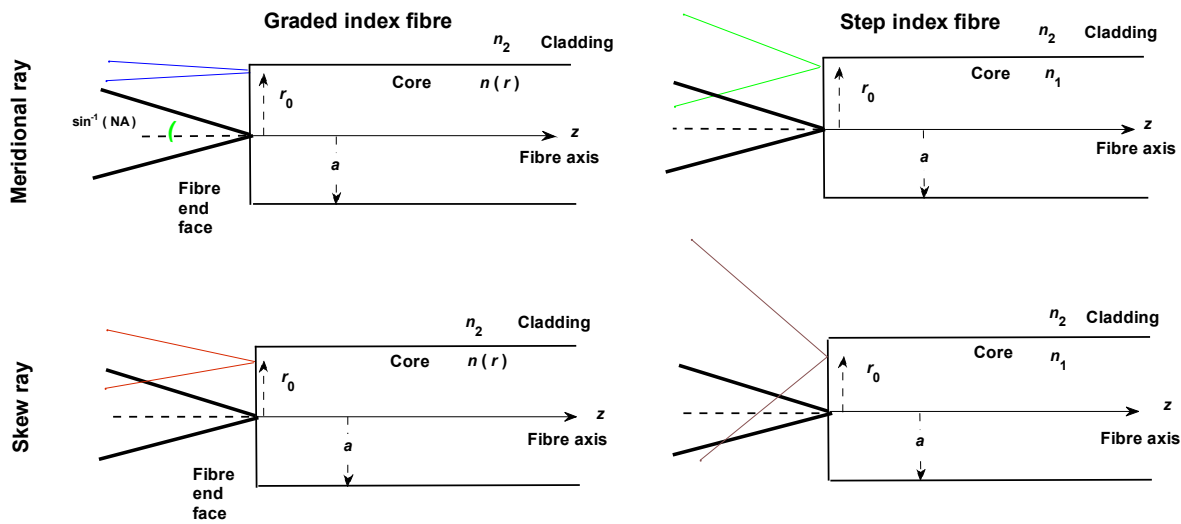


Fig. 2. 15 Side view of fibre acceptance cone (NA) for graded and step index fibres.

### 3. Simplified Wave Propagation Model in Graded Index Fibres (Eikonal Equation)

By using a different form of the Fermat's principle, we get what is called Eikonal Equation, that is

$$|\nabla S(\mathbf{R})|^2 = n^2(\mathbf{R}) \quad (3.1)$$

where  $S(\mathbf{R})$  represents the wave from surface of a quasi plane wave propagating in the fibre and  $n(\mathbf{R})$  is again the three dimensional refractive index in the medium of propagation. Like the mode analysis carried out for step index, we assume that the angular dependence is in the form of  $\exp(-j\nu\phi)$  and the axial ( $z$  axis) dependence is in the form of  $\exp(-j\beta z)$ , and the radial dependence is in the form of

$$\exp\left[-j\int_0^r k_r(\xi) d\xi\right] \quad (3.2)$$

For these components of  $S(\mathbf{R})$ , if we apply the  $\nabla$  in cylindrical coordinates

$$\nabla = \frac{\partial}{\partial r} + \frac{1}{r} \frac{\partial}{\partial \phi} + \frac{\partial}{\partial z} \quad (3.3)$$

By rewriting (3.1) as

$$k^2 |\nabla S(\mathbf{R})|^2 = k^2 n^2(\mathbf{R}) \quad (3.4)$$

we get

$$k_r^2(r) = k^2 n^2(r) - \beta^2 - \frac{\nu^2}{r^2} \quad (3.5)$$

For the radial component,  $k_r^2(r)$ , it is possible to take on positive and negative values. Positive values correspond to sinusoidal variations in (3.2), while negative values of  $k_r^2(r)$  will result in imaginary  $k_r(r)$ , then (3.2) will result in exponential decay, where the field is evanescent. It is important to note, this region of evanescence must start before we reach the core cladding boundary and never change its status. This is essential for a ray (wave) can propagate forward along  $z$  (fibre) axis. Otherwise the energy of the propagating wave will tunnel out to the cladding radially, instead of propagating forward. More specifically plotting  $k_r^2(r)$  for different cases against the normalized radial distance, we obtain the following graphs illustrated in Figs. 2.16 – 2.20. Upon examination, we see that only meridional guided (Fig. 2.16) and skew guided (Fig. 2.18) rays will propagate along the fibre axis. The remaining ones, i.e. those rays shown in Figs. 2.17, 2.19 and 2.20 will refract out to the cladding slowly (leaky) or rapidly.

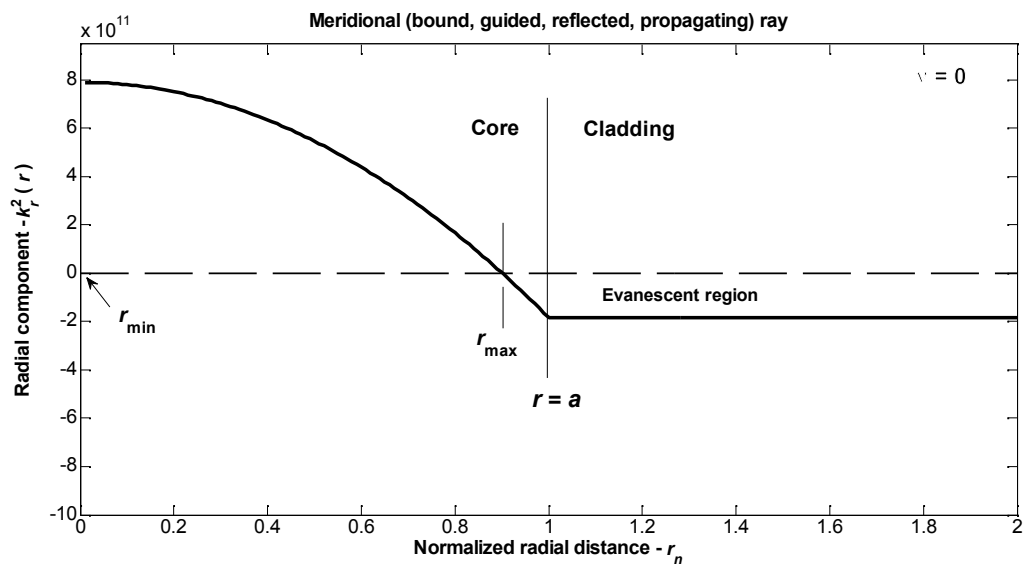


Fig. 2.16 The Radial component of a meridional guided (propagating) ray along the fibre cross section.

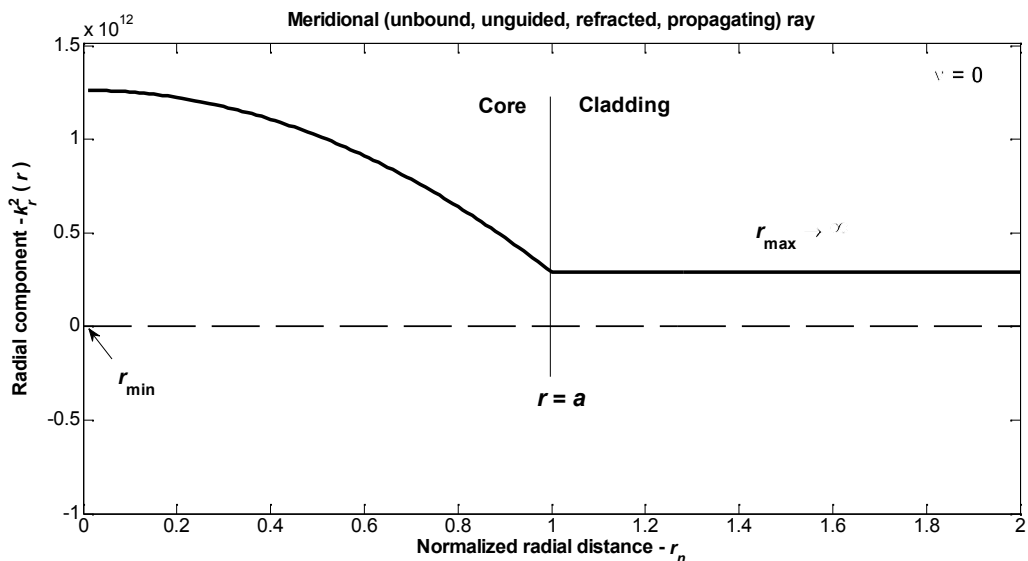


Fig. 2.17 The Radial component of a meridional unguided (refracted) ray along the fibre cross section.

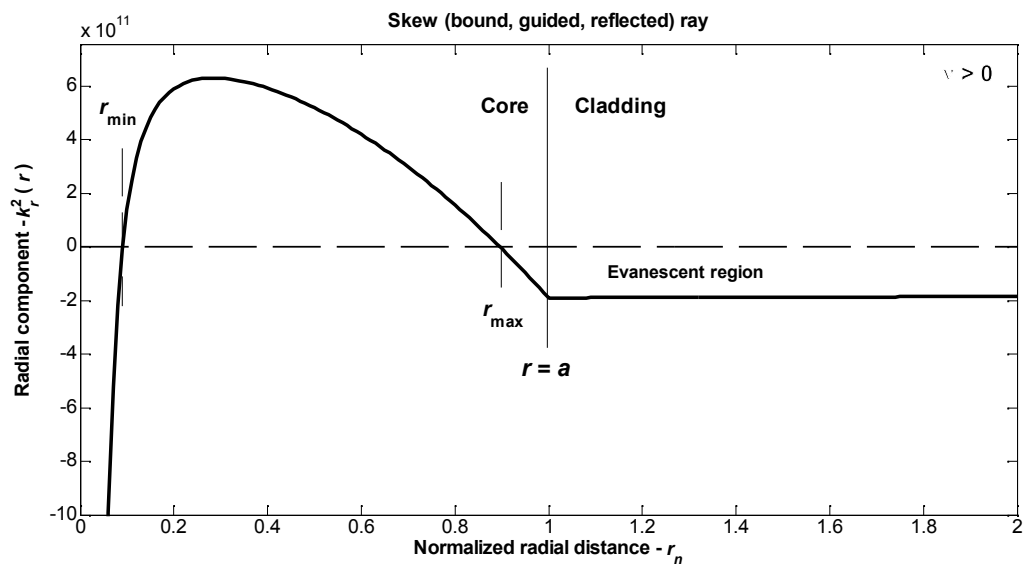


Fig. 2.18 The Radial component of a skew guided (propagating) ray along the fibre cross section.

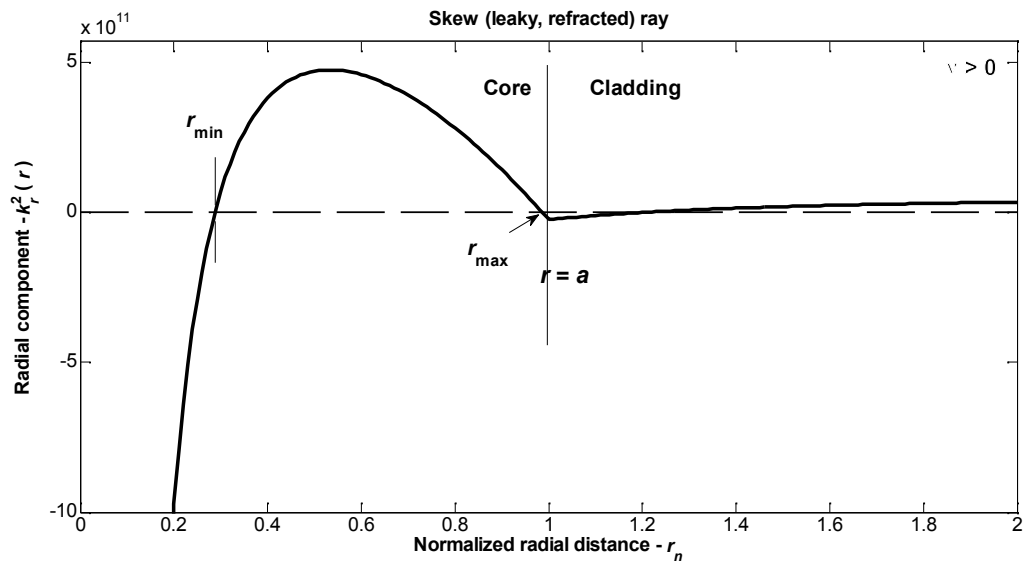


Fig. 2.19 The Radial component of a skew leaky ray along the fibre cross section.

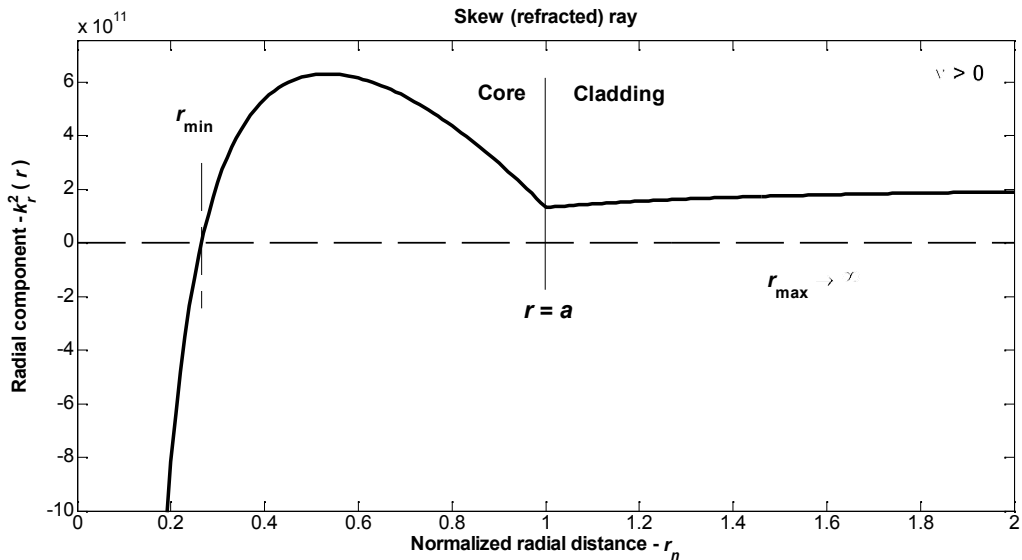


Fig. 2.20 The Radial component of a skew refracted ray along the fibre cross section.

Similar to earlier developments, as also seen from Figs. 2.16 – 2.20, in  $k_r^2(r)$  graphs, the zero crossings along the radial axis are named  $r_{\min}$  and  $r_{\max}$  which can also be found by setting (3.5) to zero. We further know from (2.26) that, the ray (wave) path is periodic, thus we can write the following

$$2 \int_{r_{\min}}^{r_{\max}} k_r(r) dr = 2\pi m \quad (3.6)$$

Upon solving the integral in (3.6) by setting  $n^2(r)$  to quadratic profile, we get

$$\frac{a(k^2 n_1^2 - \beta^2)}{4kn_1 \sqrt{2\Delta}} - \frac{\nu}{2} = m \quad (3.7)$$

It is clear from (3.7) that we can calculate the propagation constant,  $\beta$  by assigning (positive) integer values to  $\nu$  and  $m$ . For this, we rearrange (3.7) as follows

$$\beta = \left[ \frac{ak^2 n_1^2 - 4kn_1 \sqrt{2\Delta} (m + \nu/2)}{a} \right]^{0.5} \quad (3.8)$$

A related experiment with Matlab file name WKBcurves\_Exp3.m will be performed to calculate the propagation constant,  $\beta$  using (3.8) and observe the graphs of Figs. 2.16 – 2.20.

These notes are based on

- 1) Gerd Keiser, "Optical Fiber Communications" 3<sup>rd</sup> Ed. 2000, McGraw Hill, ISBN : 0-07-116468-5.
- 2) Govind P. Agrawal, "Fiber-Optic Communication Systems" 2002, Jon Wiley and Sons, ISBN : 0-471-21571-6.

- 3) B. E. A. Saleh, M.C. Teich "Fundamentals of Photonics" , 2007, Wiley, ISBN No : 978-0-471-35832-9.
- 4) H. Hatsumura, "The light acceptance angle of a graded index fibre", Optical and Quantum Electronics, 7, (1975), 81-86.
- 5) My own ECE 474 Lecture Notes.